International Journal of Automotive Technology, Vol. 5, No. 3, pp. 165–172 (2004)

1229–9138/2004/017–03

MODELING OF DIRECT INJECTION DIESEL ENGINE EMISSIONS FOR A QUASI-DIMENSIONAL MULTI-ZONE SPRAY MODEL

D. JUNG* and D. N. ASSANIS

Department of Mechanical Engineering, The University of Michigan, Ann Arbor, MI 48109-2121, U.S.A.

(Received 8 September 2003; Revised 1 April 2004)

ABSTRACT–Phenomenological models for direct injection diesel engine emissions including NO, soot, and HC were implemented into a full engine cycle simulation and validated with experimental data obtained from representative heavy-duty DI diesel engines. The cycle simulation developed earlier by Jung and Assanis (2001) features a quasi-dimensional, multi-zone, spray combustion model to account for transient spray evolution, fuel-air mixing, ignition and combustion. In this study, additional models for HC emissions were newly implemented and the models for NO, soot, and HC emissions were validated against experimental data. It is shown that the models can predict the emissions with reasonable accuracy. However, additional effort may be required to enhance the fidelity of models across a wide range of operating conditions and engine types.

KEY WORDS : Diesel, Emissions, NO, Soot, HC, Quasi-dimensional, Multi-zone model

NOMENCLATURE

A	: constant
$\bar{C}$	: average fuel mass concentration
C	: mass concentration
c	: fraction factor
E	: activation energy
H	: hydrogen
HC	: hydrocarbon
k	: forward rate constant
M	: molecular weight
m	: mass
N	: nitrogen
NO	: nitric oxide
nz	: number of zones in a parcel
O	: oxygen
OH	: hydroxyl
P	: pressure
R	: gas constant
$\bar{R}$	: universal gas constant
r	: radial distance from the center line
T	: temperature
t	: time
V	: volume
ρ	: density

SUPERSCRIPT

a	: exponent
b	: exponent

SUBSCRIPT

a	: air
c	: centerline
e	: equilibrium
exp	: expansion stroke
i	: index
f	: fuel
m	: maximum
ol	: over-leaned
op	: over-penetration
ox	: oxygen
s	: soot emitted
sac	: SAC volume
sf	: soot formed
so	: soot oxdized

1. INTRODUCTION

Compression ignition diesel engines are known to be the most efficient energy converter of fossil fuels for vehicle propulsion, with a projected thermal efficiency potential of 55%. Recently the diesel engine has been evolving

*Corresponding author. e-mail: dohoy@umich.edu

from being a rough, noisy and polluting engine to a high-tech power propulsion system. Assisted by technologies such as innovative electronic, electromagnetic, electro-hydraulic and pneumatic systems, advanced control strategies, high pressure multiple fuel injections, variable geometry turbocharger and other externally-assisted turbo-chargers with charge air cooling, exhaust gas recirculation, combustion chamber modifications, and novel aftertreatment systems, the next generation, advanced diesel engine has the potential for being not only fuel economical but also environmentally-friendly. As the available technical options for low emissions and high fuel economy increase, exploring the options through hardware experiments alone would not only be a very expensive and time-consuming proposition, but would also run the risk of not yielding a globally-optimized solution at the systems level. Therefore, development and use of advanced simulation validated against experimental data could be an efficient methodology during the development process of globally optimized engines aimed at low emissions.

Diesel engine simulation models can be classified into three categories, zero-dimensional, single-zone models, quasi-dimensional, multi-zone models and multi-dimensional models. Zero-dimensional models (e.g., Assanis and Heywood, 1986) are not appropriate to account for exhaust emissions due to the lack of spatial information. On the other hand, multi-dimensional models, like KIVA (Amsden *et al.*, 1985) resolve the space of the cylinder on a fine grid, thus providing a formidable amount of special information. However, computational time and storage constraints still restrain these codes from routine use for design purposes. As an intermediate, quasi-dimensional, multi-zone models (e.g., Hiroyasu *et al.*, 1983; Morel *et al.*, 1996; Rakopoulos *et al.*, 1998; Jung and Assanis, 2001) can be effectively used to model diesel engine combustion systems. The quasi-dimensional models combine some of the advantages of zero-dimensional models and multi-dimensional models. Unlike multi-dimensional models, only the fuel spray is divided into a number of zones, which significantly reduces computational load on calculating ambient gas conditions while still providing the spatial information enough to predict emissions products.

Jung and Assanis (2001) developed a quasi-dimensional, multi-zone, direct injection (DI) diesel combustion model. Figure 1 illustrates the development of fuel parcels and zones within parcels. Fuel injected into the combustion chamber according to the fuel injection schedule forms a parcel during each time step that moves in the spray axial direction. Each fuel parcel is further divided into small zones that are distributed in the radial direction. Each zone is considered as an open system control volume and mass, energy and species equations for each zone are solved. Instead of solving the full momentum equation,

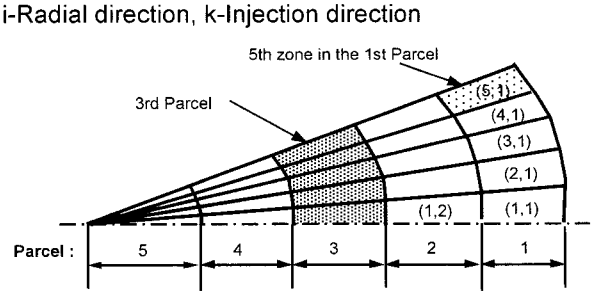

Figure 1. Division of fuel spray into parcels and zones.

which is one of the dominant reasons of computational inefficiency of multi-dimensional models, these models depend on a blend of fundamental theory, similarity considerations, and experimental data to describe spray penetration and evolution. In addition, simple momentum conservation is used to calculate the amount of air entrained into each zone. Accordingly, these models can provide the spatial information required to predict emission products and require significantly less computing resources compared to multi-dimensional models. In this study, phenomenological models for DI diesel engine emissions including nitric oxide, soot, and unburned hydrocarbon (HC) are implemented into the quasi-dimensional model and validated with experimental data obtained from representative heavy-duty, DI diesel engines. Critical sub-models, such as the heat release and emissions processes, contain empirical constants that need to be calibrated against experiments. The detail calibration process is described in (Jung and Assanis, 2001) and the same constants are used in this study. The scope of this paper is limited to the emissions models and described in the following sections.

2. POLLUTANT EMISSIONS SUBMODELS

2.1. Nitric Oxide Emissions

While nitric oxide (NO) and nitrogen dioxide are usually grouped together as NOx emissions, NO is predominant in diesel engines (Heywood, 1988). Therefore, only NO formation is considered in the present study. The principal source of NO is the oxidation of atmospheric nitrogen. The formation and destruction processes are not part of the fuel combustion process. However, the reactions that produce NO take place in an environment created by the combustion reactions, so the two processes are still intimately linked. Nitric oxide forms throughout the high-temperature burned gases behind the flame through chemical reactions involving nitrogen and oxygen atoms and molecules, which do not attain chemical equilibrium. The principal reactions governing the formation of NO from molecular nitrogen and its destruction are

(Lavoie *et al.*, 1970):

$$N+NO \xleftrightarrow{k_1} N_2+O \quad (1)$$

$$O+NO \xleftrightarrow{k_2} O_2+N \quad (2)$$

$$N+OH \xleftrightarrow{k_3} NO+H \quad (3)$$

where forward rate constants, k_1, k_2, and k_3 are in m^3/kmole/s:

$$k_1=1.6\times10^{10} \quad (4)$$

$$k_2=1.5\times10^{6}T\exp\left(-\frac{19500}{T}\right) \quad (5)$$

$$k_3=4.1\times10^{10} \quad (6)$$

This is often called the extended Zeldovich's mechanism. Zeldovich was the first to suggest the importance of reactions (1) and (2). Lavoie *et al.* (1970) added reaction (3) to the mechanism. The rate of change of NO concentration is expressed as (Heywood, 1988):

$$\frac{d[NO]}{dt}=\frac{2R_1\{1-([NO]/[NO]_e)^2\}}{1+([NO]/[NO]_e)R_1/(R_2+R_3)} \quad (7)$$

where

$$R_1=k_1[NO]_e[N]_e \quad (8)$$

$$R_2=k_2[NO]_e[O]_e \quad (9)$$

$$R_3=k_3[N]_e[OH]_e \quad (10)$$

The bracket, [ ], in Equation (7) to Equation (10) denotes species concentration in kmole/m^3. The NO formation in each zone can be calculated with Equation (7). Then total amount of NO is calculated by summing up NO formed in each zone.

2.2. Soot Formation and Oxidation

Soot forms in the rich unburned-fuel-containing core of the fuel sprays, within the flame region, where the fuel vapor is heated by mixing with hot burned gases. Soot then oxidizes in the flame zone when it contacts unburned oxygen. Therefore, the concentration of soot in the exhaust is governed by the formation and oxidation of soot during the engine cycle, i.e.

$$\frac{dm_s}{dt}=\frac{dm_{sf}}{dt}-\frac{dm_{so}}{dt} \quad (11)$$

The general fact that the net soot formation rate is primarily affected by pressure, temperature and equivalence ratio has been fairly well established. However, the details of the mechanism leading to soot formation are not known. Consequently, semi-empirical, two-rate equation models have been used to describe the soot dynamics. In particular, the soot formation model proposed by Hiroyasu *et al.* (1983) is used in many multi-zone models. The formation rate is calculated by assuming a first-order reaction of vaporized fuel, m_{fg}, as:

$$\frac{dm_{sf}}{dt}=A_f m_{fg}P^{0.5}\exp\left(\frac{-E_{sf}}{\bar{R}T}\right) \quad (12)$$

The soot oxidation is predicted by assuming a second-order reaction between soot, m_s, and oxygen.

$$\frac{dm_{so}}{dt}=A_o m_s\frac{P_{ox}}{P}P^{1.8}\exp\left(\frac{-E_{so}}{\bar{R}T}\right) \quad (13)$$

where $E_{sf}=5.23\times10^4$ kJ/kmol, $E_{so}=5.86\times10^4$ kJ/kmol. A_f and A_o are constants that are determined by matching the calculated soot with the measured data in the exhaust gas. Total amount of soot is obtained by summing up soot mass calculated with Equation (11) in each zone.

2.3. Hydrocarbon Emissions

The incomplete combustion of internal combustion engines powered by hydrocarbon fuel results in the hydrocarbon emissions. Among the factors that cause HC emissions from diesel engines, the fuel over-leaned beyond combustion limit and under-mixing of fuel from the nozzle SAC volume at low velocity after the completion of injection are the most important reasons under normal operating conditions (Heywood, 1988). In addition to those, the effect of wall quenching due to spray over-penetration cannot be ignored in case of small DI diesel engines (Matsui *et al.*, 1987; Kuo *et al.*, 1988). At light load and idle, over-mixing is especially important, particularly in engines of relatively small cylinder size at high speed. Cyclic misfire and local under-mixing influence HC emissions only under extreme operating conditions like cold start or extended idling so, these effects are not included in this study.

Phenomenological modeling of three major sources of HC emissions: (1) leaned-out fuel during the ignition delay, (2) fuel yielded by the SAC volume and nozzle hole, and (3) over-penetrated fuel, is presented in the following sub-sections.

2.3.1. The effect of over-mixining

Some of the fuel injected into the combustion chamber during the ignition delay period is vaporized and mixed with air beyond the lean limit of equivalence ratio, ϕ_l. While the over-leaned fuel can escape the primary combustion process unburned or only partially reacted, thermal oxidation of some of these hydrocarbons can occur during the expansion process. The value of ϕ_l will be determined by the lean limit for flammability or by the lean limit for self-ignition (whichever gives the lower value of ϕ_l) at the prevailing pressures (3–10 MPa) and temperature (800–1500 K) of the lean mixtures in the diesel combustion chamber. Under these conditions the lean flammability limit is expected to be the order of ϕ =0.1–0.3 and to be relatively insensitive to the range of

temperatures and pressures at present of interest. The data on lean limit for self-ignition suggest a similar insensitivity to the range of temperatures and pressures of interest so that as a first approximation it can be assumed that ϕ_l is constant (Greeves *et al.*, 1977). The lean limit is assumed 0.2 in this study.

The first step for the calculation of the HC emissions from the over-leaned mixture is to estimate the over-leaned fuel at the start of combustion. It is approximately order of 1% of fuel injected during that period. The problem with multi-zone spray model on this is that multi-zone model cannot calculate the amount of over-leaned fuel precisely unless the spatial resolution is high enough to distinguish the portion of over-leaned fuel spray. Increasing resolution will increases computational load. So, a different approach is proposed in this study instead of increasing zonal resolution to avoid any computational cost. The average fuel concentration of a parcel, which is a set of zones introduced to the combustion chamber at a given time step, can be calculated using the information from the multi-zone spray model as followed.

$$\bar{C}=\frac{\sum_{i=1}^{nz} m_{f,i}}{\sum_{i=1}^{nz} m_{f,i}+\sum_{i=1}^{nz} m_{a,i}} \tag{14}$$

where $m_{f,i}$ and $m_{a,i}$ denote the mass of fuel and air of the i-th zone in a parcel, respectively and nz is the number of zones in a parcel. The fuel concentration profile for each parcel is assumed as Yu *et al.* (1980) proposed.

$$\frac{C(r)}{C_c}=1-\left(\frac{r}{r_m}\right)^{1.5} \tag{15}$$

By knowing the radius of the spray and the average fuel concentration of a parcel, the fuel concentration at the centerline can be calculated from Equation (15) and accordingly the fuel distribution. Then the mass of over-leaned fuel can be obtained for each parcel.

Some of the over-leaned fuel is then oxidized during the expansion process. In general, the reaction rate can be represented in the form of

$$\frac{d[HC]}{dt}=-A_1[HC]^a[O_2]^b\exp\left(\frac{-E}{\bar{R}T}\right) \tag{16}$$

The constant A_1 is in units of $(m^3/kmole)^{a+b}sec^{-1}$.

As for spark ignition (SI) engines, HC oxidation rates have been determined in a number of different studies and several different empirical correlations of the data in the form of overall reaction rate equations under exhaust gas conditions (near stoichiometric air-fuel ratio and atmospheric pressure) have been proposed (Lavoie, 1978). However, correlations for diesel-like conditions are rare. Furthermore the correlations for SI engines cannot be applied to the diesel engine cases since the fuel composition, conditions and processes of HC emissions formation in the diesel engines are substantially different. For the over-leaned condition, the variation of the concentration of the oxygen will be very small (Greeves *et al.*, 1977) so, a simplified expression of the following form is assumed:

$$\frac{d[HC]}{dt}=-A_2[HC]^a\exp\left(\frac{-E}{\bar{R}T}\right) \tag{17}$$

By using the following relation,

$$[i]=\frac{m_i}{M_i V} \tag{18}$$

Equation (17) can be rewritten as

$$\frac{dm_{HC}}{dt}=-A_3\frac{m_{HC}^a}{V}\exp\left(\frac{-E}{\bar{R}T}\right) \tag{19}$$

where A_3 is 1.161×10^{11}; a is 2; and E is 7.79×10^4 kJ/kmol.

Total mass of the over-leaned fuel of each parcel at the start of combustion is used as the initial value of HC for the time integration of Equation (19). And the final HC emissions from the over-leaned fuel can be obtained by integrating Equation (19) for the expansion stroke:

$$m_{HC,ol}=\int_{\exp}\frac{dm_{HC}}{dt} \tag{20}$$

2.3.2. The effect of SAC and nozzle hole volume

As the valve is closed at the end of the injection period the injection pressure decreases rapidly, and right after the valve is closed the pressure in the SAC volume could be lower than the cylinder pressure. Consequently, some fuel remained in the SAC and nozzle holes. However, the SAC volume is not always completely full of fuel due to cavities induced by low pressures in the SAC when injection terminates rapidly. The remained fuel then issues at a very low rate from the nozzle SAC with relatively low momentum energy forming large liquid drop after a delay from the main injection. It evaporates and mixes very slowly and hence the corresponding mixture element is fuel rich until too late in the engine cycle. Therefore, most of the fuel from the SAC and hole volume is assumed to appear as HC emissions.

The SAC and nozzle hole volume is not fully filled with fuel due to the cavity as mentioned in the previous section. To include the cavity effect, a fraction factor is introduced as in Equation (21). The value of the fraction factor, c_{sac}, is assumed as 0.12 due to Lakshminarayanan *et al.* (Lakshminarayanan *et al.*, 2000).

$$m_{HC,sac}=c_{sac}\rho_f V_{sac} \tag{21}$$

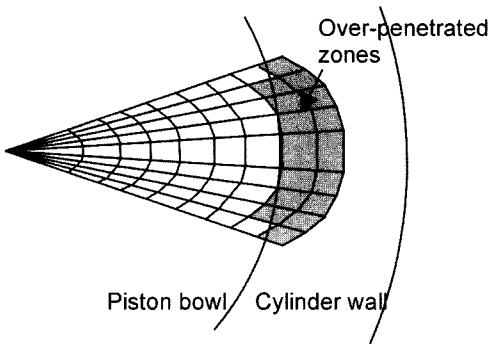

Figure 2. Over-penetrated fuel spray.

2.3.3. The effect of over-penetration

In case of large-bore engines, the over-leaned fuel during the ignition delay period and under-mixed fuel from the SAC and nozzle holes after the injection are known to be the major sources of HC emissions (Greeves *et al.*, 1977; Yu *et al.*, 1980). However, Kuo *et al.* (1988) found that the contribution of the over-leaned fuel to HC emissions in a smaller bore engines could be only 10 to 30% of the total HC emissions. Another significant source of HC emissions from small diesel engines applied to passenger cars is identified as the HC emissions from the over-penetrated fuel. The over-penetrated fuel includes the fuel vapor deflected by the walls, the liquid fuel rebounded from the walls, and the liquid fuel stuck on the walls. A part of the over-penetrated fuel will be consumed in the combustion process. However, the remainder of the impinging fuel, especially the fraction stuck on the combustion chamber surface could potentially be emitted from the engine as HC emissions. This could account for 0 to 65 percent of the total HC emissions from the engine that they examined. Correlation of the over-penetrated fuel with the measured HC indicated that approximately 2% of the fuel mass that over penetrated before start of combustion exhibits itself as unburned HC emissions.

Because of the difficulty of decomposing the over-penetrated fuel into individual components, all of the over-penetrated fuel was used to quantify the extent of wall impingement. To calculate the mass of over-penetrated fuel, the zones are allowed to penetrate without the restriction of wall boundary, then the zones passed beyond the walls are considered as over-penetrated zones. Figure 2 illustrates this. The mass of over-penetrated fuel is the summation of fuel mass of over-penetrated zones. Accordingly HC emissions due to over-penetration is given by

$$m_{HC,op}=c_{op}\sum_{i=op}^{zones} m_{f,i} \tag{22}$$

where c_{op} is fraction of over-penetrated fuel that emitted as HC emissions, which is 0.02.

Table 1. Engine specifications and data availability.

Engine	DDC 60	CAT 3406
Type	Multi-cyl.	Single-cyl.
Bore (mm)	130	137
Stroke (mm)	160	165
Comp. ratio (–)	15	15
Rated speed (rpm)	2100	2100
Rated power (kW)	350	54

3. MODEL VALIDATION

3.1. Experimental Data

NO and HC Emissions predictions of multi-zone model have been compared against corresponding measurements on a in-line, six cylinder, turbocharged, inter-cooled, water-cooled, direct injection diesel engine at the Automotive Research Center located in the University of Michigan. Additional validation of the multi-zone model's predictions was conducted using reported data from an independent engine set-up at the Engine Research Center of the University of Wisconsin (Nehmer *et al.*, 1994). This work on a modern single-cylinder, four-diesel stroke engine was selected for the completeness in reporting soot and NO emissions over a range of injection timings. Primary specifications of the engines are listed in Table 1. The multi-cylinder engine has relatively quiescent combustion chamber with a shallow "Mexican hat" bowl-in piston and produces very high injection pressures, delivered by unit injectors. The fuel injection timing and duration are electrically controlled. The single cylinder engine set-up is based on a version of the Caterpillar 3406 production engine with simulated turbocharging, and is capable of producing 54 kW at a rated speed of 2100 rpm.

3.2. Nitric Oxide Emissions

To verify the accuracy of the model over a wide range of operating conditions, predicted NO emissions were compared with experimental data acquired on the multi-cylinder engine for a range of loads varying from 10% to

Table 2. Operating conditions.

Parameter	Value
Engine speed (rpm)	1600
Equivalence ratio	0.45
Injection timing (δεγ. BTDC)	5, 8, 11, 13, 15
Inlet air temperature (deg. C)	36
Inlet air pressure (kPa)	184
Exhaust back pressure (kPa)	159

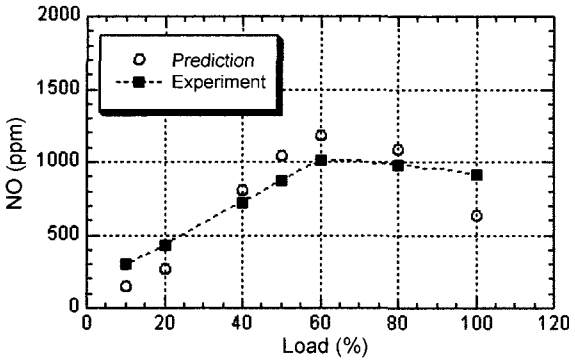

Figure 3. Predicted and measured NO emissions over a range of loads at 2100 rpm (Multi-cylinder engine).

100%, at a speed of 2100 rpm in Figure 3. As can be seen in Figure 3, the model predicted exact trend of NO variation with the change of engine load and showed quantitatively good agreement with experimental data. The fidelity of the model has been explored further by comparing its predictions with data over a range of speeds at constant load. Engine speed has been varied from 900 to 2100 rpm in increments of 300 rpm. Load

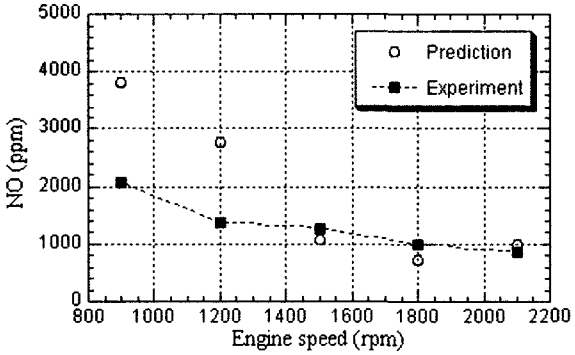

Figure 4. Predicted and measured NO emissions over a range of speeds at 50% loads (Multi-cylinder engine).

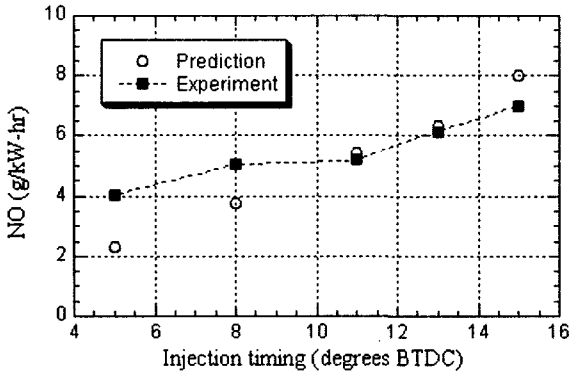

Figure 5. Predicted and measured NO emissions over a range of injection timings (Single-cylinder engine).

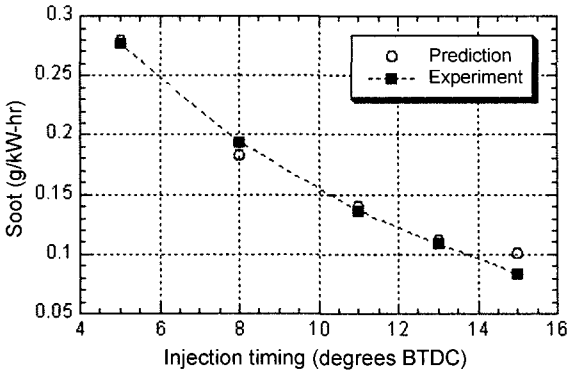

Figure 6. Predicted and measured soot emissions over a range of injection timings (Single-cylinder engine).

was set at 50%. The result was shown in Figure 4. The model was able to predict the trend correctly, however, it overpredicted NO at low engine speeds.

Following model validation with the multi-cylinder engine, more extensive comparison of predictions with measurements from the single cylinder engine was carried out over a range of injection timings. The operating conditions are listed in Table 2. The conditions were chosen to reflect common loads placed on the engine (1600 rpm and equivalence ratio of 0.45, or approximately 80% load), as well as the appropriate inlet temperature and pressure conditions. Predictions of emissions are compared with experimental data for injection timings of 5, 8, 11, 13 and 15 deg. BTDC. Predicted and measured NO emissions were compared in Figure 5. The model predicted trend correctly, however, it underpredicted NO at retarded injection timings.

3.3. Soot Formation and Oxidation

For the soot model, the pre-exponential constant, A_f, in Equation (12) is set here at 150, which is, the same value used by Patterson *et al.* (1994). The other pre-exponential constant, A_o, in Equation (13) is calibrated (A_o=2250) to match the soot level with measurements under the baseline operating condition (11 degree BTDC). Comparisons of predicted soot emissions with measurements from the single cylinder engine were carried out over a range of injection timings (from 5 to 15 degrees CA BTDC). As sown in Figure 6, the predicted values are in excellent agreement with measurement.

3.4. Hydrocarbon Emissions

HC emissions model was validated against experimental data acquired on the multi-cylinder engine for a range of engine loads and speeds as done for NO emissions model validation. Figure 7 shows the comparison of predicted and measured HC emissions over a range of loads at 2100 rpm. As can be seen in Figure 7, the model predicted

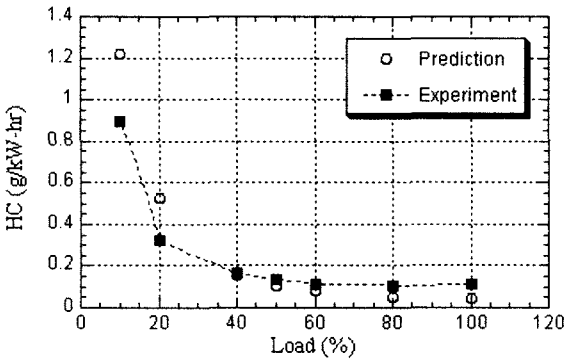

Figure 7. Predicted and measured HC emissions over a range of loads at 2100 rpm (Multi-cylinder engine).

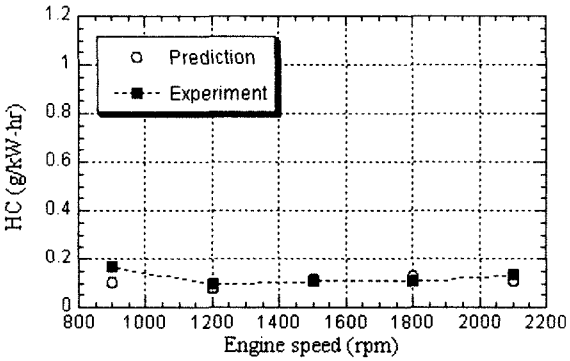

Figure 8. Predicted and measured HC emissions over a range of speeds at 50% loads (Multi-cylinder engine).

exact trend of HC variation with the change of engine load and showed quantitatively very good agreement with experimental data. The model showed the capability of predicting HC accurately over the range of engine speeds as shown in Figure 8.

In Figure 9, the contribution of the sources to HC emissions was compared. The results showed that there was no effect of over-penetration observed expect 10% load condition. In other words, the fuel spray did not reach the walls during the ignition delay period in most cases simulated here. This is reasonable because the tested engine is relatively large-sized heavy-duty engine, Even though the effect of over-penetration was not quantitatively demonstrated over a range here, it is very important to verify if the spray reached the wall. Quantitative validation of over-penetration effect on HC emissions would be possible with smaller size diesel engines and remained to be done. Figure 9 shows that over-mixing effect during the ignition delay period is the most dominant source of HC emissions in this case. The nozzle of the engine tested is VCO type, which has no SAC volume. Accordingly, HC emissions due to SAC and hole volume are smaller than the HC caused by over-mixing effect.

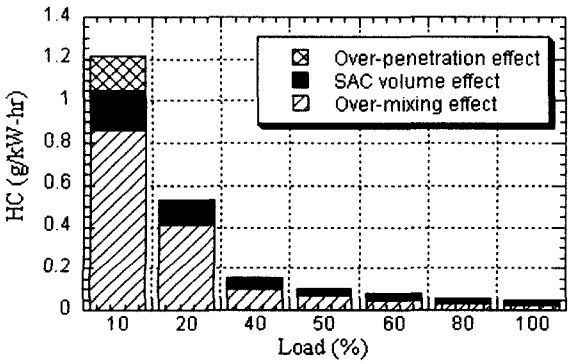

Figure 9. Sources of HC emissions over a range of loads at 2100 rpm (Multi-cylinder engine).

4. CONCLUSIONS

Phenomenological models for DI diesel engine emissions including NO, soot, and HC are implemented into a full engine cycle simulation based on quasi-dimensional multi-zonal spray combustion model. A comprehensive validation of the proposed models against experimental data obtained from representative heavy-duty DI diesel engines has been conducted over a range of injection pressures, injection timings, engine speeds and engine loads. The major conclusions are the following:

- NO model predicted exact trends of NO variation with the change of engine loads, speeds and injection timings of both multi- and single cylinder engines. The comparison of predicted and measured data demonstrated reasonable agreement between them quantitatively.
- Predicted soot emissions with semi-empirical, two-rate equation models over a range of injection timings showed excellent agreement with measurement from the single cylinder engine.
- The following three major sources of HC emissions are modeled in this study: (1) leaned-out fuel during the ignition delay, (2) fuel yielded by the SAC volume, and (3) over-penetrated fuel.
- The model showed the capability of predicting HC accurately over the range of engine speeds and loads. The specific engine examined for HC emissions in this study revealed that the fuel spray did not over-penetrated in most cases.
- Additional effort is required to enhance the fidelity of each model across a wide range of operating conditions and engine types including high-speed small diesel engines.

ACKNOWLEDGEMENT–The authors would like to acknowledge the technical and financial support of the Automotive Research Center (ARC) by the National Automotive Center (NAC) located within the US Army Tank-

Automotive Research, Development and Engineering Center (TARDEC). The ARC is a U.S. Army Center of Excellence for Automotive Research at the University of Michigan, currently in partnership with 7 other universities nationwide. Timothy Jacobs, and Dr. Zoran Filipi are gratefully acknowledged for providing data acquired on the ARC heavy-duty engine test cell for model validation.

REFERENCES

Amsden, A. A., Ramshaw, J. D., ORourke, P. J. and Dukowicz, J. K. (1985). KIVA: A computer program for two- and three-dimensional fluid flow with chemical reactions and fuel sprays. *Los Alamos National Laboratory Report* LA-10245-MS.

Assanis, D. N. and Heywood, J. B. (1986). Development and use of a computer simulation of the turbocompounded diesel system for engine performance and component heat transfer studies. *SAE Paper No.* 860329.

Greeves, G., Khan, I. M., Wang, C. H. T. and Fenne, I. (1977). Origins of hydrocarbon emissions from diesel engines. *SAE Paper No.* 770259.

Heywood, J. B. (1988). *Internal Combustion Engine Fundamentals*. McGraw-Hill Book. Inc. New York.

Hiroyasu, H., Kadota, T. and Arai, M. (1983). Development and use of a spray combustion modeling to predict diesel engine efficiency and pollutant emissions (Part 1 Combustion modeling). *Bulletin of the JSME* **26**, **214**, 569–575.

Jung, D. and Assanis, D. N. (2001). Multi-zone DI diesel spray combustion model for cycle simulation studies of engine performance and emissions. *SAE Transactions: Journal of Engines* **110**, **3**, 1510–1532.

Kuo, T.-W., Wu, K.-J. and Henningsen, S. (1988). Effects of fuel overpenetration and overmixing during ignition delay period on hydrocarbon emissions from a small open-chamber diesel engine. *J. Eng. Gas Turbines and Power* **110**, **3**, 453–461.

Lakshminarayanan, P. A., Nayak, N., Dingare, S. V. and Dani, A. D. (2000). Predicting HC emissions from DI diesel engines. *ASME Paper No.* 2000-ICE-327.

Lavoie, G. A., Heywood, J. B. and Keck, J. C. (1970). Experimental and theoretical investigation of nitric oxide formation in internal combustion engines. *Combust. Sci. Technol.* **1**, 313–326.

Lavoie, G. A. (1978). Correlations of combustion data for S.I. engine calculations-laminar flame speed, quench distance and global reaction rates. *SAE Paper No.* 780229.

Matsui, Y. and Sugihara, K. (1987). Sources of hydrocarbon emissions from a small direct injection diesel engine. *SAE Paper No.* 871613.

Morel, T. and Wahiduzzaman, S. (1996). Modeling of diesel combustion and emissions. *96 FISITA Proceedings*, 26th International Congress, Praha, Czech Republic, June 17–21.

Nehmer, D. A. and Reitz, R. D. (1994). Measurement of the effect of injection rate and split injections on diesel engine soot and NOx emissions. *SAE Paper No.* 940668.

Patterson, M. A., Kong, S. C., Hampson, G. J. and Reitz, R. D. (1994). Modeling the effects of fuel injection characteristics on diesel engine soot and NOx emissions. *SAE Paper No.* 940523.

Rakopoulos, C. D. and Hountalas, D. T. (1998). Development and validation of a 3-D multi-zone combustion model for the prediction of DI diesel engines performance and pollutants emissions. *SAE Paper No.* 981021.

Yu, R. C., Wong, V. W. and Shahed, S. M. (1980). Sources of hydrocarbon emissions from direct injection diesel engines. *SAE Paper No.* 800048.